DOI: 10.1002/ejic.201100268

New Insights in the Formation of Combined Zeolitic/Mesoporous Materials by using a One-Pot Templating Synthesis

Jarian Vernimmen,[a] Vera Meynen,[a] Sebastiaan J. F. Herregods,[a,b] Myrjam Mertens,[b] Oleg I. Lebedev,[c,d] Gustaaf Van Tendeloo,[d] and Pegie Cool*[a]

Keywords: Zeolites / Mesoporous materials / Hydrothermal synthesis / Composites / One-pot templating synthesis

Zeolitic growth is often absent or occurs in separate phases when synthetic strategies based on the combination of zeolite templates and mesopore templating agents are applied. In this work, zeolitic growth and mesopore formation have been investigated at different temperatures by applying a one-pot templating approach, based on a TS-1 zeolite synthesis whereby part of the microtemplate (tetrapropylammonium hydroxide, TPAOH) is replaced by a mesotemplate (hexadecyltrimethylammonium bromide, CTMABr). Moreover, the synthesis duration and the molar ratio of the microtemplate/mesotemplate have also been studied. The different syntheses clearly show the inherent competitive mechanism between zeolitic growth and mesopore formation. These insights have led to the conclusion that by following a one-pot templating strategy with standard, nonexotic commercial templates, i.e. CTMABr and TPAOH, it is not possible to develop a "true" hierarchical mesoporous zeolite, meaning a mesoporous siliceous material with highly crystalline zeolitic walls. The resultant materials are instead combined zeolitic/mesoporous composite structures with, however, highly tuneable and controllable porosity characteristics.

Introduction

During the last decade, research into siliceous materials chemistry has been focused on the synthesis of combined zeolitic/mesoporous materials.[1] These structures are considered as very useful and promising since they have the potential to combine (i) the enhanced diffusion and accessibility for larger molecules and viscous fluids of mesoporous materials with (ii) the remarkable stability, catalytic activity and selectivity of zeolites. A lot of different synthetic strategies have already been developed in order to create these types of materials such as recrystallisation,[2] carbon-based methods[3] and template-assisted approaches.[4] The absolute goal of these syntheses is to develop a hierarchical mesoporous zeolite, meaning a siliceous material with controlled mesoporosity and highly crystalline, zeolitic walls. A frequently studied synthetic approach is the one-pot templating synthesis,[5] whereby scientists are attempting to simultaneously create mesoporosity and zeolitic features by mixing the silica source (and the heteroelement source), a zeolite structure directing agent and mesotemplate in one reaction vessel. The main idea behind this approach is to have an in situ formation of zeolitic particles that organise around the mesotemplate micelles. For example, Karlsson et al.[5c] used a mixture of C6/C14TMABr (alkyltrimethylammonium bromide) to synthesise MFI/MCM-41 composites. Poladi et al.[5b] described the preparation of Ti-MMM-1, a mixed phase MCM-41 and MFI material, in which the organic templates for the meso- and micropores are added at staggered times to the reaction mixture. In the majority of these syntheses, focus is put on the characteristics of the materials, the synthetic procedure and the often enhanced catalytic performance of these materials compared with their purely zeolitic or mesoporous counterparts.[5a,5b,5d] Although several successes have been observed, much less attention has been paid to the formation mechanism of the combined zeolitic/mesoporous materials and to the location of the zeolitic and mesoporous phase: (1) separate phases; (2) connected phases but with single zeolitic domains embedded in the mesoporous matrix or (3) "true" hierarchical structures with zeolitic features in the mesopore walls (micro- and mesopores are interconnected). Consequently, although these types of materials often give rise to improved catalytic activity, it remains unclear whether the one-pot templating syntheses using standard, nonexotic commercial templates can lead to "true" hierarchical mesoporous zeolites, whereby the zeolitic domains build up the mesopores instead of resulting in zeolitic/mesoporous composites. Moreover, it is also unclear whether

[a] Laboratory of Adsorption and Catalysis, Department of Chemistry, University of Antwerp,
Universiteitsplein 1, 2610 Wilrijk, Belgium
Fax: +32-3-265-23-74
E-mail: pegie.cool@ua.ac.be
[b] VITO - Flemish Institute for Technological Research - NV, Boeretang 200, 2400 Mol, Belgium
[c] CRISMAT, UMR 6508, CNRS-ENSICAEN, 6 Bd Marechal Juin, 14050 Caen, France
[d] EMAT, University of Antwerp, Groenenborgerlaan 171, 2020 Antwerpen, Belgium
Supporting information for this article is available on the WWW under http://dx.doi.org/10.1002/ejic.201100268.

more exotic and expensive templates, such as silylated surfactants, are a necessity to achieve "true" hierarchical mesoporous zeolites.[6]

In this report, we discuss the results of investigating the zeolitic growth and the formation of the mesoporous structure by applying a one-pot templating synthesis, based on a TS-1 zeolite recipe,[7] using a micro- and a mesotemplate (TPAOH and CTMABr, respectively). All materials were thoroughly characterised by a wide range of techniques, namely N_2 sorption, thermogravimetric analysis, FTIR and UV/Vis (DR) spectroscopy, XRD, elemental analysis and TEM. We have shown that it is not possible to obtain a "true" hierarchical mesoporous zeolite by simply replacing part of the microtemplate (TPAOH) by a mesotemplate (CTMABr). It will be demonstrated that the zeolite formation is inhibited by the presence of a mesopore templating agent. Moreover, the temperature that is needed to obtain a zeolitic phase is unfavourable for the mesostructure itself. However, the ideal combination of temperature and duration of the hydrothermal treatment (HT) and ratio of micro- and mesotemplate leads to zeolitic/mesoporous composite materials with interesting properties that can be tuned towards a dominant mesoporous structure on the one hand or a pronounced zeolitic structure on the other.

Results and Discussion

Influence of the Mesopore Templating Agent CTMABr on the Zeolite Formation

In Figure 1 the N_2 sorption isotherms of TS-1-2d-100 °C-100% zeolite, TS-1-2d-100 °C-50% zeolite and meso-TSM-2d-100 °C materials are shown. Note that except for the fact that the TS-1 zeolites are synthesised with a template concentration of 100% or 50% TPAOH compared with 50% TPAOH and 50% CTMABr for meso-TSM-2d-100 °C, the synthetic conditions of all materials are exactly the same. The isotherms clearly show that meso-TSM-2d-100 °C is a mesoporous material (type IV isotherm according to IUPAC classification) whereas TS-1-2d-100 °C-100% and TS-1-2d-100 °C-50% are microporous (type I isotherms). The porosity characteristics of the materials are summarised in Table 1. These data indicate that meso-TSM-2d-100 °C has a high specific surface area, high total pore volume and no microporosity whereas TS-1-2d-100 °C-100% and TS-1-2d-100 °C-50% are microporous and both have a specific surface area and total pore volume representative for a TS-1 zeolite.[8] It is noteworthy that the amount of added microtemplate, TPAOH, has no influence on the quality of the zeolite structure, since in both cases (50% and 100% TPAOH), a full-grown TS-1 zeolite is formed (see also the XRD pattern in Figure 1, inset). This observation points out that the structural differences between TS-1-2d-100 °C-*z*% (*z* = 50 or 100) and meso-TSM-2d-100 °C are due to the mesotemplate CTMABr and are not related to a difference in TPAOH concentration. Therefore, from these three syntheses, it is clear that only when the mesotemplate CTMABr is added to the synthetic mixture, mesopores are formed. However, this does not guarantee the existence of any hierarchical structuring.

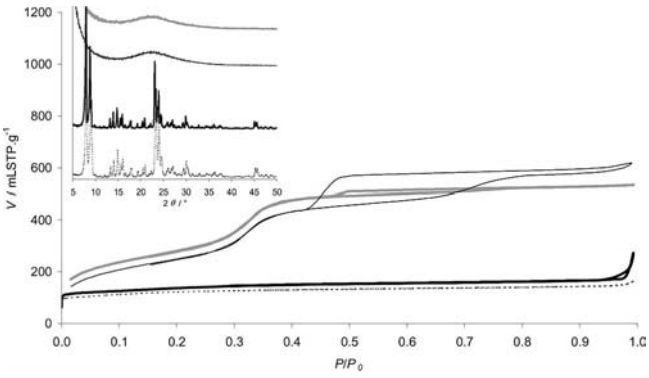

Figure 1. N_2 sorption isotherms and XRD patterns (inset) in the region 5–50° 2θ [in offset] of TS-1-2d-100 °C-100% (dotted black line), TS-1-2d-100 °C-50% (bold black line), meso-TSM-2d-100 °C (grey line) and meso-TSM-4d-100 °C (black line).

Table 1. Porosity data and Ti-content of Ti-incorporated siliceous materials.

	Wt.-% Ti	BET[a] /$m^2 g^{-1}$	V_μ[b] /$mL g^{-1}$	V_{tot}[c] /$mL g^{-1}$	Ø[d] /nm
TS-1-2d-100 °C-100%	2.9	434	0.18	0.23	–
TS-1-2d-100 °C-50%	3.0	496	0.22	0.26	–
TS-1-2d-150 °C-100%	3.2	452	0.17	0.24	–
meso-TSM-2d-100 °C	1.7	967	0.00	0.83	2.8
meso-TSM-4d-100 °C	1.7	918	0.00	0.93	2.8
meso-TSM-2d-125 °C	1.8	861	0.00	0.76	2.8
meso-TSM-2d-150 °C	2.0	709	0.00	0.62	2.8
meso-TSM-4d-150 °C	1.6	569	0.00	0.59	3.5
meso-TSM-7d-150 °C	1.7	372	0.00	0.39	4.0

[a] Specific surface area. [b] Micropore volume. [c] Total pore volume at P/P_0 = 0.98. [d] Average pore diameter, based on the adsorption PSD.

The zeolitic features of the materials were studied by XRD (Figure 1, inset) and only in the cases of TS-1-2d-100 °C-100% and TS-1-2d-100 °C-50% is a MFI zeolite profile visible. Meso-TSM-2d-100 °C shows a broad band between 15° and 35° for 2θ which is typical for amorphous materials. Even though at 100 °C the zeolite can be formed, it seems that the zeolite formation at 100 °C is completely disrupted in the presence of the mesotemplate CTMABr. Moreover, even when the duration of the HT of meso-TSM-2d-100 °C is prolonged, the resultant material (meso-TSM-4d-100 °C) is still a purely mesoporous material (Figure 1, Table 1) with no zeolitic features visible from XRD (Figure 1, inset). Also TGA and DRIFT show no zeolitic features for the meso-TSM-2d-100 °C and meso-TSM-4d-100 °C materials as no weight loss occurs around 390 °C due to incorporated TPAOH. Furthermore, the characteristic IR band due to the MFI pentasil ring vibration at 550 cm^{-1} is absent as well (Supporting Information, Figure S1 and S2).[9] These four syntheses clearly show that the zeolite formation is inhibited in the presence of the mesotemplate CTMABr. Thus, at 100 °C the affinity or kinetics of the silica- and the titanium source condensation around

the mesotemplate is higher than for the zeolite structure directing agent (TPAOH). Therefore, under these circumstances, it can be concluded that is not possible to obtain a hierarchical or even a composite zeolitic/mesoporous material since the zeolite formation does not take place.

Factors Determining the Formation of a Combined Zeolitic/Mesoporous Material

To determine whether increasing the temperature of the HT can induce zeolitic growth in the presence of CTMABr and lead to the formation of a combined zeolitic/mesoporous material, meso-TSM-2d-125 °C and meso-TSM-2d-150 °C were synthesised. The XRD-patterns (Figure 2) of the materials show that on the one hand, meso-TSM-2d-100 °C and meso-TSM-2d-125 °C give rise to a broad band between 15° and 35° 2θ, which is typical for amorphous materials (Figure 2b). On the other hand, meso-TSM-2d-150 °C has a sharp diffraction typical for TS-1, superimposed on a broad signal between 15 and 35° 2θ, indicating the presence of both zeolitic as well as amorphous character. The region between 0 and 6° 2θ provides information about the mesophase ordering (Figure 2a). Here, all three meso-TSM materials show two peaks at 1.9° and 4.1° 2θ, which suggest a hexagonal structure (MCM-41). It is, however, not perfectly hexagonally ordered throughout the entire structure since the higher order reflections [(110), (200) and (210)] are not well resolved or absent (only 2 instead of 4 peaks are observed).[10] This does not imply that these structures cannot be valuable in certain applications, since the ordering of the pores is often less relevant than a high porosity and a uniform pore size. It is clear that the temperature is of primordial importance for the zeolitic growth in the presence of CTMABr as it directly controls the extent of the zeolitic character of the meso-TSM materials.

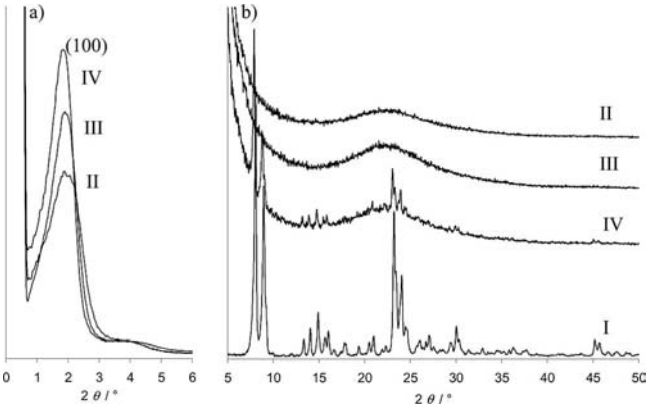

Figure 2. XRD patterns in the region (a) 0–6° 2θ [enlargement: 46×] and (b) 5–50° 2θ [in offset] of TS-1-2d-150 °C-100% (I), meso-TSM-2d-100 °C (II), meso-TSM-2d-125 °C (III) and meso-TSM-2d-150 °C (IV).

The direct correlation between the temperature and zeolitic properties can also be observed by thermogravimetric analysis (Figure 3). Here, only meso-TSM-2d-150 °C has a small weight loss at 390 °C which indicates the presence of incorporated TPAOH, thus zeolitic character. All other materials have only CTMABr in their structure, corresponding to the two weight losses between 180 °C and 340 °C which are similar to the ones in conventional MCM-41.[11] DRIFT (4a) also confirms the zeolitic character of meso-TSM-2d-150 °C: it is the only meso-TSM material that has a small band at 550 cm^{-1} which has been assigned to the pentasil ring vibration of a MFI zeolite.[9] The FTIR band at 1050 cm^{-1} (Figure 4a and enlarged in Figure 4b) is slightly shifted to higher wavenumbers when the temperature is higher than 100 °C, meaning that the Si–O–Si bond strength increases due to shortening of the silicate bonds and this is due to a better condensation at elevated temperature.[12] The grey arrow is the peak maximum of meso-TSM-2d-100 °C, whereas the black arrow indicates that of meso-TSM-2d-125 °C and meso-TSM-2d-150 °C. The differences observed in the FTIR spectra are small, but significant. Therefore, DRIFT reveals that the degree of condensation of the meso-TSM structure increases with increasing temperature. This enhanced condensation can also be an indication for increasing zeolitic character with increasing temperature, although no zeolitic features are yet observed at 125 °C. At higher temperature, meso-TSM-2d-150 °C shows some zeolitic features (DRIFT: band at 550 cm^{-1} and an enhanced condensation due to increasing zeolitic character; XRD: clear MFI profile) but they are still quite different from the full-grown TS-1 zeolite as evidenced by a major contribution of the amorphous phase (XRD and DRIFT) and a relatively small weight loss in TGA around 390 °C. Despite these clear indications for zeolitic character of meso-TSM-2d-150 °C, the micropore volume calculated by the *t*-plot method is zero (Table 1). This can be explained by the fact that (i) the zeolitic part is quite small and / or (ii) the zeolite crystal sizes are so minuscule that they are calculated as part of the external surface area. The observations derived from the different characterisation techniques clearly show that it is difficult to unambiguously investigate the zeolitic features of a combined zeolitic /mesoporous material solely based on one technique. Moreover, based on the techniques applied thus far in this work, it is very difficult to unambiguously determine whether the resultant material is a zeolitic / mesoporous composite or a "true" hierarchical mesoporous zeolite.

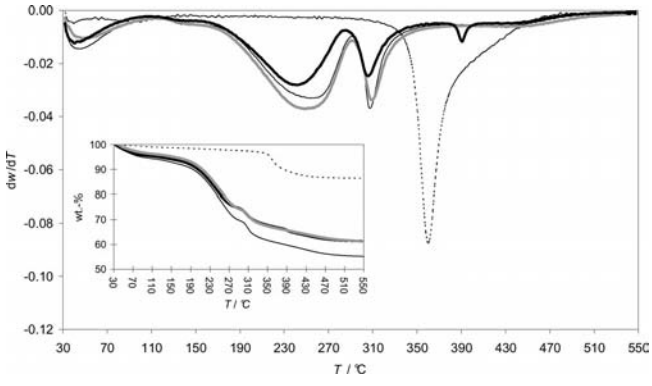

Figure 3. DTG and TG curve (inset) of TS-1-2d-150 °C-100% (dotted black line), meso-TSM-2d-100 °C (black line), meso-TSM-2d-125 °C (grey line) and meso-TSM-2d-150 °C (bold black line).

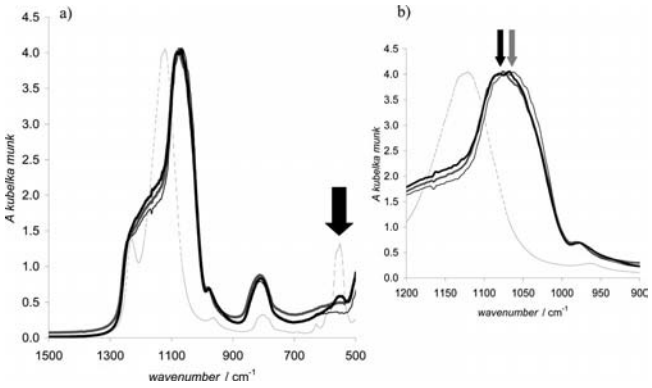

Figure 4. (a and b): FTIR spectra of TS-1-2d-150 °C-100% (dotted black line), meso-TSM-2d-100 °C (black line), meso-TSM-2d-125 °C (grey line) and meso-TSM-2d-150 °C (bold black line).

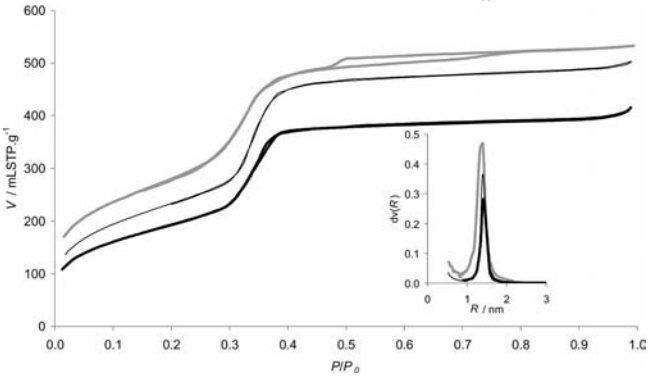

Figure 5. N_2 sorption isotherms and adsorption pore size distributions of meso-TSM-2d-100 °C (grey line), meso-TSM-2d-125 °C (black line) and meso-TSM-2d-150 °C (bold black line).

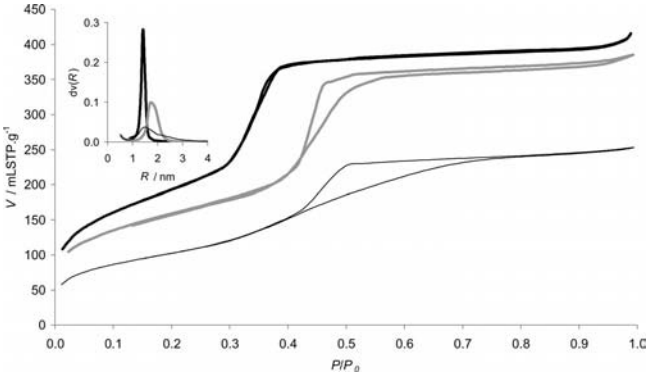

Figure 6. N_2 sorption isotherms and adsorption pore size distribution (inset) of meso-TSM-2d-150 °C (bold black line), meso-TSM-4d-150 °C (grey line) and meso-TSM-7d-150 °C (black line).

Not only is the zeolitic character strongly influenced by the temperature of the HT, the mesostructure is affected as well. The N_2 sorption isotherms (Figure 5) of the meso-TSM materials are all of type IV according to IUPAC classifications and correspond in shape to that of MCM-41. In addition, meso-TSM-2d-100 °C has a small triangular hysteresis loop between P/P_0 = 0.45 and 0.75, indicating the presence of a secondary slit-shaped mesoporosity. The maximum of the PSD is not influenced by the temperature and the PSD curves remain narrow. This indicates that the pores have a constant size with a high degree of uniformity. On the other hand, the specific surface area and total pore volume decrease with increasing temperature of the HT (Table 1). The appearance of zeolitic properties and the degradation of the mesoporous structure at higher temperature strongly suggest that the formation of the zeolitic part, even in the small quantity observed here, is at the expense of the mesostructure. This decrease in mesoporous characteristics at a temperature of 150 °C becomes even more important when the duration of the HT is prolonged from two to seven days. Figure 6 depicts the N_2 sorption isotherms and adsorption PSDs of meso-TSM-2d-150 °C, meso-TSM-4d-150 °C and meso-TSM-7d-150 °C. Although all three materials give rise to a type IV isotherm, the quality of the mesoporous structure is clearly a function of the duration of the HT. The change in the mesoporous structures with an increasing hydrothermal period can be derived from the shape of the isotherms, the less steep capillary condensation, the increase in pore dimensions (shift of the capillary condensation step and PSD average) and the broadening of the PSD curves indicating less uniform pores. Also the specific surface area and the total pore volume decrease with increasing length of the HT (Table 1).

The enlargement of the pore diameter and eventual degradation of the mesostructure at longer hydrothermal treatments at 150 °C can be related to the decomposition of the mesotemplate CTMABr into DMHA (dimethylhexadecylammonium bromide, a swelling agent). For MCM-41 structures, it is well documented that CTMABr can (partially) decompose into DMHA in basic conditions at a temperature ≥ 150 °C (similar to the synthetic conditions applied here).[13] Therefore, in the meso-TSM materials, long hydrothermal treatments at 150 °C will cause the loss of CTMABr and lead to an increased swelling of the pore sizes as more DMHA is being formed in situ with increasing duration. Moreover, while the mesoporous ordering decreases, the zeolitic features increase upon prolonging the HT: in XRD (Supporting Information, Figure S3), the intensity of the zeolitic peaks increases with increasing length of the HT, suggesting that there are more and/or larger zeolitic particles after seven days than after two and four days. In addition, TGA (Supporting Information, Figure S4) shows that the amount of incorporated TPAOH increases with prolonged HT which also reflects the growing zeolitic character of the meso-TSM materials. However, at the same time, the weight loss due to CTMABr (180–340 °C) decreases. Therefore, the growth of zeolite crystals can be controlled by the duration of the HT at 150 °C but this also coincides with a loss of mesoporosity, indicating a gradual transformation of the mesostructure into a zeolitic phase. However, when the temperature of the HT is below 150 °C, the resultant materials do not show zeolitic features in XRD, even if the duration of the HT is prolonged to seven days (Supporting Information, Figure S5). Zeolitic growth in the presence of a mesotemplate thus only appears when the temperature is high enough (150 °C). Unfortunately,

Table 2. Porosity data of meso-TSM materials, synthesised with a different ratio of microtemplate/mesotemplate; hydrothermal treatment of 2 days at 150 °C.

% TPAOH/% CTMABr	TPAOH/ CTMABr	BET[a] /$m^2 g^{-1}$	V_μ [b] /$mL g^{-1}$	V_{tot}[c] /$mL g^{-1}$	Ø[d] /nm
60%/40%	1.5	384	0.07	0.23	–
70%/50%	1.4	379	0.04	0.25	–
60%/50%	1.2	644	0.00	0.59	3.2
50%/45%	1.1	654	0.00	0.67	2.9
50%/50%	1.0	709	0.00	0.62	2.8
60%/65%	0.9	640	0.00	0.71	3.2
60%/75%	0.8	738	0.00	0.66	3.0

[a] Specific surface area. [b] Micropore volume. [c] Total pore volume at $P/P_0 = 0.98$. [d] Average pore diameter, based on the adsorption PSD.

this also implies that the quality of the mesostructure will deteriorate. These results clearly indicate the competition between mesopore formation and zeolitic growth.

In order to further investigate this competition between zeolite and mesopore formation, meso-TSM materials were synthesised with a variation in the molar ratio of the microtemplate/mesotemplate. Table 2, Figure 7a and 7b show the effect of adjusting the molar ratio of microtemplate/mesotemplate for an HT of two days at 150 °C (reminder: meso-TSM-2d-150 °C = 50% TPAOH / 50% CTMABr). The results show that a trade-off needs to be reached between a high mesoporosity and zeolitic character. When the TPAOH / CTMABr ratio is lower than 1.0, the materials are highly mesoporous but they hardly show any zeolitic features in XRD. On the contrary, when much more TPAOH than CTMABr is added to the synthetic mixture (ratio of 1.5 and 1.4), the resultant materials give rise to a type I isotherm reflecting their microporous / zeolitic nature. Moreover, their zeolitic features are very prominent in XRD, meaning that these materials have evolved into full-grown TS-1 zeolites. When applying a ratio between 1.0 and 1.2, a good compromise between a high mesoporosity and zeolitic features can be made. In particular, the 50% TPAOH / 50% CTMABr meso-TSM material has a high specific surface area and very uniform mesopores in combination with zeolitic character in XRD. From these syntheses, it is clear that a proper tuning of the microtemplate / mesotemplate ratio is crucial in obtaining a material with a high mesoporosity as well as zeolitic character. Moreover,

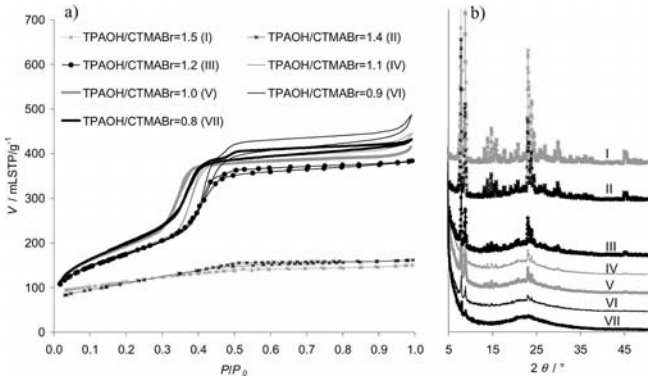

Figure 7. (a) N_2 sorption isotherms and (b) XRD results [in offset] of meso-TSM materials, synthesised with different microtemplate/mesotemplate ratios.

these experiments point out that there is quite a narrow range of microtemplate / mesotemplate ratios in which it is possible to create a combined zeolitic / mesoporous siliceous material. A ratio between 1.0 and 1.2 seems to be very critical in order to obtain a material with a high mesoporosity as well as pronounced zeolitic character. Moreover, as discussed in previous paragraphs, a temperature of 150 °C is required to obtain any zeolitic character. When deviating from this narrow range, the resultant material will be either a full-grown zeolite or a purely mesoporous material even at 150 °C. These experiments further emphasise the competitive behaviour of zeolite and mesopore formation as discussed in earlier paragraphs.

"True" Hierarchical Mesoporous Zeolites or Not?

HRTEM is the ultimate technique for determining whether a combined zeolitic/mesoporous material is a composite structure with separate zeolitic phases and mesoporous parts or a "true" hierarchical mesoporous material with zeolitic walls. Synthesised meso-TSM materials with both zeolitic features as well as mesoporosity were subjected to a HRTEM study. Figure 8 depicts some representative HRTEM images of meso-TSM-2d-150 °C. Here, the small zeolitic MFI particles [± 20 nm] (Figure 8a) lie at the edges of the mesoporous phase which is partly hexagonally ordered and partly worm-like (Figure 8b). These HRTEM images demonstrate that even the most optimal material, i.e. the material with zeolitic features while still retaining a highly mesoporous structure (meso-TSM-2d-150 °C), is a composite and not a "true" hierarchical mesoporous zeolite. EDX measurements (not shown, see Table 1 for the Ti-content) illustrate that the active centres (Ti) are spread throughout the entire structure and are not only located in the zeolitic parts. Even though part of the Ti-content is located in the amorphous phase, according to UV-DR analysis, the coordination of Ti is predominantly tetrahedral (Supporting Information, Figure S6). This could be beneficial for redox reactions with large molecules that require tetrahedrally coordinated titanium. Meso-TSM-4d-150 °C and meso-TSM-7d-150 °C show similar TEM results, reflecting their composite structures (not shown here). The presence of separate mesoporous and zeolitic phases is not so surprising knowing the here described underlying competition in interaction between zeolite and mesopore forma-

tion. Therefore, we conclude that by applying a one-pot templating strategy, whereby solely standard, nonexotic, commercial templates, i.e. TPAOH and CTMABr, are involved, the competitive growth mechanism between the zeolite and mesophase will inhibit the formation of a "true" hierarchical mesoporous zeolite. The resultant materials will be zeolitic / mesoporous composites instead with, however, highly tuneable porosity characteristics that can be directed towards dominant zeolitic or mesoporous properties that can definitely be valuable for certain applications. However, if "true" hierarchical mesoporous zeolites are required, more expensive, exotic tailor-made templates, such as silylated surfactants, are recommended.

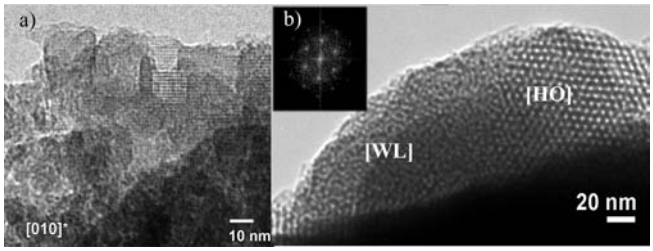

Figure 8. HRTEM images of meso-TSM-2d-150 °C with (a) zeolitic particles at the edges of the mesostructure and (b) a mesophase partly hexagonally ordered [HO] and partly worm-like [WL]. The FT pattern is given as an insert and shows hexagonal symmetry.

Conclusions

In this paper, the zeolitic growth and formation of the mesostructure in the synthesis of combined zeolitic / mesoporous materials have been studied by applying a one-pot templating strategy, based on a TS-1 zeolite recipe whereby part of the microtemplate (TPAOH) is replaced by a mesotemplate (CTMABr). All materials have been thoroughly characterised by N_2 sorption, XRD, TGA, FTIR, UV/Vis (DR), EPMA and TEM. The influence of the synthetic temperature, duration and microtemplate / mesotemplate ratio has been investigated and led to important insights in the formation mechanism of combined zeolitic / mesoporous materials. At a temperature of 100 °C, it has been shown that the formation of the zeolitic phase is hampered in the presence of the mesotemplate CTMABr. A higher temperature of 150 °C is needed to obtain zeolitic features. However, long hydrothermal treatments at 150 °C will lead to a degraded mesostructure due to the decomposition of CTMABr and gradual transformation of the mesoporous structure into a zeolitic phase. Moreover, the microtemplate / mesotemplate ratio is another crucial parameter in the one-pot templating synthesis which can really tune the porosity characteristics of the resultant materials towards a dominant mesoporous structure or pronounced zeolitic character. Because of the competitive growth mechanism of the zeolitic phase and mesostructure, a trade-off needs to be reached between high mesoporosity and pronounced zeolitic character. Optimisation of the different synthetic parameters (hydrothermal treatment for two days at 150 °C and molar ratio of microtemplate / mesotemplate = 1.0–1.2) led to the formation of interesting combined zeolitic / mesoporous materials. These materials are not "true" hierarchical mesoporous zeolites, meaning a siliceous material whereby the zeolitic parts build up the mesopores but instead zeolitic / mesoporous composites. Summarising, this study showed that due to the competition of the zeolite and mesopore formation, a one-pot templating synthesis, using standard, nonexotic, commercially available zeolite structure directing agents and mesotemplates, i.e. TPAOH and CTMABr, will not be able to provide "true" hierarchical mesoporous zeolites but will inherently lead to zeolitic / mesoporous composite materials. Nevertheless, this does not exclude that these type materials with highly tuneable characteristics can be very valuable in sorption, separation and catalytic applications.

Experimental Section

Chemicals: Tetraethylorthosilicate (TEOS, 98%), titaniumbutoxide (TBOT) and hexadecyltrimethylammonium bromide (CTMABr) were purchased from Acros. Tetrapropylammonium hydroxide (TPAOH, 1.0 M solution in water) was purchased from Aldrich.

Syntheses

Titanium-incorporated siliceous materials were prepared by an adjusted synthesis for the titanium-silicalite-1 (TS-1) zeolite.[7] In the TS-1 zeolite synthesis, part of the zeolite structure directing agent (TPAOH) was replaced by a mesopore templating agent (CTMABr). The molar ratio of micro- and mesotemplate was 1:1 (50% TPAOH / 50% CTMABr) in all the syntheses, unless stated differently. The overall concentration of templates was kept the same as in the original synthesis of the zeolite (TPAOH + CTMABr = 100 mol-%). This led to a mixture with an initial molar ratio of 1 TBOT / 30 TEOS / 4 TPAOH / 4 CTMABr / 1050 H_2O. Note that in all the syntheses, TPAOH has a double function, namely to act as a microtemplate and as a base. A typical synthetic procedure is described as follows: CTMABr (1.4 g) was dissolved in distilled water (13.5 mL). TPAOH (3.75 mL) was then added to the surfactant solution with stirring. Following this, TBOT (300 μL) and TEOS (5.6 mL) were added with vigorous stirring. After a stirring period of 1.5 h at room temperature, the mixture was subjected to hydrothermal treatment (HT) of 100, 125 or 150 °C with a variable length (2, 4 or 7 days). After filtering, washing and drying of the final product, a calcination procedure was carried out. The materials were calcined in an ambient atmosphere at 550 °C for 6 h with a heating rate of 1 °C min^{-1}.

The materials are denoted as meso-TSM-*x*d-*y*°C, whereby *x* represents the length of the HT [2, 4 or 7 days)] and *y* the temperature of the HT [100–125–150 °C]. *TS* originates from *t*itanium-*s*ilicalite-1 and *M* is derived from CT*M*ABr.

Full-grown TS-1 zeolites were made as references. The TS-1 synthesis was applied[7] without addition of a mesotemplate, followed by a HT. These TS-1 zeolites are denoted as TS-1-*x*d-*y*°C-*z*%, whereby *x* represents the duration of the HT in days, *y* the temperature of the HT and *z* the amount of added TPAOH in molar percentage (100% means 1 TBOT / 30 TEOS / 8 TPAOH / 1050 H_2O, whereas 50% is 1 TBOT / 30 TEOS / 4 TPAOH / 1050 H_2O). The characteristics of the prepared zeolites fully agree with those described in

the Atlas of Zeolite Framework Types and in the Collection of Simulated XRD Powder Patterns for Zeolites of the International Zeolite Association.[14]

Characterisation Techniques

The N_2 sorption measurements at –196 °C were determined using a Quantachrome Quadrasorb SI automated gas sorption system. Prior to measurements, the samples were degassed in vacuum for 16 h at a temperature of 200 °C. The Barret-Joyner-Halenda (BJH) method applied on the adsorption branch of the isotherm was used to determine the pore size distribution (PSD). The micropore volume was obtained by means of the *t*-plot method, while the Brunauer-Emmet-Teller (BET) method was applied to calculate the specific surface area. The total pore volume was determined at $P/P_0 = 0.98$.

Electron probe microanalysis (EPMA) was utilised for the determination of the titanium concentration in the samples. The EPMA analyses were performed on a JEOL JXA 733 apparatus. The coordination of titanium was determined by using a UV/Vis spectrophotometer (Thermo Electron Evolution 500), equipped with an integrating sphere (RSA-UC-40 diffuse reflectance cell). The average of three scanning cycles was taken with a scanning speed of 120 nm min^{-1} and a bandwidth of 2 nm.

Thermogravimetric analysis results were recorded on a Mettler Toledo TGA/SDTA851 instrument. The analyses were performed in an oxygen atmosphere, whereby the samples were heated from 30 °C to 550 °C with a heating rate of 5 °C min^{-1}.

Diffuse Reflectance Infrared Fourier Transform (DRIFT) spectroscopy measurements were recorded on a Nicolet 20 DXB Fourier Transform IR spectrometer equipped with a DTG detector. The samples were diluted with KBr (2% sample, 98% KBr). The resolution was set to 4 cm^{-1} and 200 scans were averaged. All measurements were performed under a flow of dry air.

X-ray diffraction (XRD) measurements were carried out on a PANalytical X′PERT PRO MPD diffractometer with Cu-radiation. A bracket stage, monochromator and soller slits were also used. The measurements were performed in the 2θ mode using a monocrystal with a scanning speed of 0.04° 4s^{-1} and measuring in continuous mode.

The meso-TSM materials were further characterised by transmission electron microscopy (TEM) and EDX analysis using a Philips CM20 microscope equipped with an Inca X-ray microanalysis unit, operating at 200 kV and a Technai G2 microscope, operating at 200 kV. The TEM samples were prepared by crushing the material in methanol in an agate mortar and dropping this dispersion of finely ground material onto a holey carbon film supported on a Cu grid. Low electron beam intensities and low magnification were applied in order to minimise the e-beam damage of the material. Fourier transformation (FT) of high resolution TEM (HRTEM) images was performed using the Digital Micrograph 3.3. software.

Supporting Information (see footnote on the first page of this article): DTG and TG curves, DRIFT spectra, XRD diffractograms, UV-DR spectra.

Acknowledgments

J. V. thanks the Fund for Scientific Research – Flanders (FWO-Vlaanderen) for financial support. The Concerted Research Project (CRP, GOA-project) sponsored by the Special Fund for Research at the University of Antwerp is acknowledged.

[1] a) K. Egeblad, C. H. Christensen, M. Kustova, C. H. Christensen, *Chem. Mater.* **2008**, *20*, 946–960; b) V. Meynen, P. Cool, E. F. Vansant, *Microporous Mesoporous Mater.* **2007**, *104*, 26–38; c) J. Pérez-Ramirez, C. H. Christensen, K. Engblad, C. H. Christensen, J. C. Groen, *Chem. Soc. Rev.* **2008**, *37*, 2530–2542; d) R. Chal, C. Gérardin, M. Bulut, S. van Donk, *ChemCatChem* **2011**, *3*, 67–81.

[2] A. A. Campos, L. Dimitrov, C. R. da Silva, M. Wallau, E. A. Urquieta-González, *Microporous Mesoporous Mater.* **2006**, *95*, 92–103.

[3] A. Sakthivel, S.-J. Huang, W.-H. Chen, Z.-H. Lan, K.-H. Chen, T.-W. Kim, R. Ryoo, A. S. T. Chiang, S.-B. Liu, *Chem. Mater.* **2004**, *16*, 3168–3175.

[4] K. Lin, Z. Sun, S. Lin, D. Jiang, F.-S. Xiao, *Microporous Mesoporous Mater.* **2004**, *72*, 193–201.

[5] a) L. Huang, W. Guo, P. Deng, Z. Xue, Q. Li, *J. Phys. Chem. B* **2000**, *104*, 2817–2823; b) R. H. P. R. Poladi, C. C. Landry, *Microporous Mesoporous Mater.* **2002**, *52*, 11–18; c) A. Karlsson, M. Stöcker, R. Schmidt, *Microporous Mesoporous Mater.* **1999**, *27*, 181–192; d) S. M. Solberg, D. Kumar, C. C. Landry, *J. Phys. Chem. B* **2005**, *109*, 24331–24337.

[6] a) M. Choi, H. S. Cho, R. Srivastava, C. Venkatesan, D.-H. Choi, R. Ryoo, *Nat. Mater.* **2006**, *5*, 718–723; b) R. Rajendra, M. Choi, R. Ryoo, *Chem. Commun.* **2006**, 4489–4491; c) V. N. Shetti, J. Kim, R. Srivastava, M. Choi, R. Ryoo, *J. Catal.* **2008**, *254*, 296–303.

[7] X. Meng, D. Li, X. Yang, Y. Yu, S. Wu, Y. Han, Q. Yang, D. Jinag, F.-S. Xiao, *J. Phys. Chem. B* **2003**, *107*, 8972–8980.

[8] M. Taramasso, G. Perego, B. Notari US Patent 4,410,501, **1983**.

[9] T. Armaroli, F. Milella, B. Notari, R. J. Willey, G. Busca, *Top. Catal.* **2001**, *15*, 63–71.

[10] J. S. Beck, J. C. Vartuli, W. J. Roth, M. E. Leonowicz, C. T. Kresge, K. D. Schmitt, C. T.-W. Chu, D. H. Olson, E. W. Sheppard, S. B. McCullen, J. B. Higgins, J. L. Schlenker, *J. Am. Chem. Soc.* **1992**, *114*, 10834–10843.

[11] X. S. Zhao, G. Q. Lu, A. K. Whittaker, G. J. Millar, H. Y. Zhu, *J. Phys. Chem. B* **1997**, *101*, 6525–6531.

[12] O. Collart, P. Van Der Voort, E. F. Vansant, D. Desplantier, A. Galarneau, F. Di Renzo, F. Fajula, *J. Phys. Chem. B* **2001**, *105*, 12771–12777.

[13] a) M. Kruk, M. Jaroniec, A. Sayari, *J. Phys. Chem. B* **1999**, *103*, 4590–4598; b) A. Sayari, M. Kruk, M. Jaroniec, I. L. Moudrakovski, *Adv. Mater.* **1998**, *10*, 1376–1379; c) C.-F. Cheng, W. Zhou, D. H. Park, J. Klinowski, M. Hargreaves, L. F. Gladden, *J. Chem. Soc. Faraday Trans.* **1997**, *93*, 359–363; d) R. Mokaya, *Microporous Mesoporous Mater.* **2001**, *44–45*, 119–127.

[14] a) Ch. Baerlocher, W. M. Meier, D. H. Olson in *Atlas of Zeolite Framework Types*, Elsevier, Amsterdam, **2001**, pp. 184–185; b) M. M. J. Treacy, J. B. Higgins in *Collection of Simulated XRD Powder Patterns for Zeolites*, Elsevier, Amsterdam, **2001**, pp. 236–237.

Received: March 17, 2011
Published Online: August 17, 2011

